Download on the App Store

LEVEL-SET APP

Simulation and Animation of Isothermal-Front Propagation in Multiscale Transient Periodic Flow

R. C. Aldredge, PhD, PE
Professor of Mechanical and Aerospace Engineering
University of California, Davis, CA, aldredge@ucdavis.edu

BACKGROUND

The Level-Set App can be used to compute and display solutions of the advection-propagation (AP) equation below, which describes the evolution of the scalar distribution $G(\mathbf{x},t)$ and the motion of its isoscalar surfaces, which are advected at the local flow velocity $\mathbf{U}(\mathbf{x},t)$ while propagating relative to the flow at the speed S_N in the direction of its normal $\mathbf{n}(\mathbf{x},t) \equiv \nabla G / |\nabla G|$.

$$\frac{\partial G}{\partial t} + (\mathbf{U} - S_N \mathbf{n}) \cdot \nabla G = 0 \tag{1}$$

Markstein & Squire [1] were the first to use this equation to describe the advection and propagation of flame surfaces, with a particular isoscalar of G defining the spatial location of a flame surface propagating normal to itself into the reactants while being advected by the flow. A form of Eq. (1) describing general interface motion was introduced earlier [2]. The AP equation has been employed in many analytical studies of flame-front stability (e.g., [1, 3-5]) and used by others [6-8] to investigate interface propagation in turbulent flow. Osher & Sethian [9] developed the first stable numerical methods for the solution of the equation for front propagation in quiescent flow. Eq. (1) is currently more generally known as the level-set equation, governing the evolution of a level-set function G the isoscalars (level sets) of which represent surfaces moving with the velocity $d\mathbf{x}/dt$ locally. The AP equation is a special case in which $d\mathbf{x}/dt \equiv \mathbf{U} - S_N \mathbf{n}$, with S_N representing the local normal propagation speed of a particular level set (e.g., the "zero level set", corresponding to $G = 0$) and $\mathbf{U}$ representing the velocity of its advection by the flow locally.

In general, S_N depends on local properties of the advection field $\mathbf{U}$ (*e.g.*, the strain rate) and the scalar distribution G (*e.g.*, the surface curvature) [1, 3, 5, 7, 9-24]. However, the Level-Set app assumes Huygens propagation, for which S_N is assumed constant and equal to the laminar-flame speed S_L with which an adiabatic planar flame would propagate through the given reactant mixture.

The Level-Set app can be used to solve the AP equation for the evolution in time of flame-surface area resulting from the corrugation of the flame by a prescribed transient multi-scale periodic excitation flow through which the flame propagates. This is of interest because the fractional increase in the burning speed of the flame above the planar-flame speed S_L is a result of

and equal to the fractional increase in the flame-surface area above the planar-flame area caused by the excitation flow [5].

FLOW-FIELD DESCRIPTION

As in earlier studies [6, 25, 26], the excitation flow prescribed in the AP equation is assumed to have the mean speed S_L along the mean direction (x) of quasi-planar flame propagation and to satisfy Taylor's hypothesis:

$$\mathbf{U}\left(\mathbf{x},t\right) \equiv S_L \hat{\mathbf{e}}_x + \mathbf{u}(x - S_L t, y, z) \tag{2}$$

Introducing the decomposition specified in Eq. (2) into Eq. (1) and transforming to the nondimensional coordinates $(\overline{\mathbf{x}}, \overline{t})$ of a reference frame moving at the mean flow-field velocity S_L gives

$$\frac{\partial \overline{G}}{\partial \overline{t}} + \overline{\mathbf{u}}(\overline{\mathbf{x}}) \cdot \overline{\nabla}\, \overline{G} = \left| \overline{\nabla}\, \overline{G} \right|, \qquad \overline{\mathbf{x}} \equiv \left(\overline{x}, \overline{y}, \overline{z}\right) \tag{3}$$

where the overbars denote nondimensionalization according to $\overline{x} \equiv (x - S_L t)/L$, $\overline{y} \equiv y/L$, $\overline{z} \equiv z/L$, $\overline{\nabla} \equiv L\nabla$, $\overline{t} \equiv t S_L/L$, $\overline{\mathbf{u}} \equiv \mathbf{u}/S_L$ and $\overline{G} \equiv G/L$; where L is the width of the computational domain, assumed to be the same along each of the coordinates in the transverse plane perpendicular to the direction of mean flame propagation. Eq. (3) is solved computationally in the Level-Set app, subject to the following initial and boundary conditions.

$$\left.\begin{aligned} \overline{G}(\overline{\mathbf{x}}, \overline{t} = 0) &= \overline{x} \\ \overline{G}(|\overline{\mathbf{x}} - \overline{\mathbf{x}}_f| > \gamma, \overline{t}) &= \gamma\, sign(\overline{G}) \\ \overline{G}(\overline{x}, \overline{y} = 1, \overline{z}, \overline{t}) &= \overline{G}(\overline{x}, \overline{y} = 0, \overline{z}, \overline{t}) \\ \overline{G}(\overline{x}, \overline{y}, \overline{z} = 1, \overline{t}) &= \overline{G}(\overline{x}, \overline{y}, \overline{z} = 0, \overline{t}) \end{aligned}\right\} \tag{4}$$

These conditions define an initially planar flame in the transverse plane $(\overline{y}, \overline{z})$ as the zero level set $(\overline{G} = 0)$. Negative values of $\overline{G}$ correspond to regions of reactant flow upstream of the propagating flame, while positive values correspond to regions containing combustion products. Periodic conditions are satisfied by $\overline{G}$ on the domain boundaries along the $(\overline{y}, \overline{z})$ axes, while $\overline{G}$ is prescribed a maximum (minimum), constant value of γ $(-\gamma)$ in product (reactant) regions sufficiently far away from the flame location $(\overline{\mathbf{x}}_f)$, in order to facilitate the reinitialization of $\overline{G}$ during the computational simulation to achieve $|\,\overline{\nabla}\, \overline{G}\,| = 1$ near the flame surface for improved accuracy.

Both monochromatic and multi-scale solenoidal excitation flows may be considered in the Level-Set app, with $\overline{\mathbf{u}} = \mathbf{u}_N/S_L$ as defined below representing an excitation having N disparate scales. The monochromatic excitation ($\mathbf{u}_1$) is the same as that considered by Aldredge [25].

$$\mathbf{u}_{\mathrm{N}} = \begin{Bmatrix} u \\ v \\ w \end{Bmatrix} \equiv \frac{2\sqrt{2}u'}{\sqrt{N}} \sum_{n=1}^{N} \begin{Bmatrix} \cos(2k_n\overline{x})\sin(k_n\overline{y})\sin(k_n\overline{z}) \\ -\sin(2k_n\overline{x})\cos(k_n\overline{y})\sin(k_n\overline{z}) \\ -\sin(2k_n\overline{x})\sin(k_n\overline{y})\cos(k_n\overline{z}) \end{Bmatrix}; \quad u' \equiv \sqrt{\tfrac{1}{3}\left\langle \mathbf{u}_N \cdot \mathbf{u}_N \right\rangle} \tag{5}$$

Here, $k_n \equiv 2^n\pi$ and u' is the intensity of excitation-flow fluctuations, with the $\langle\ \rangle$ operator denoting spatial averaging over the entire computational domain. Fig. 1 shows the distribution of the component u at $\overline{x} = 1/64$ and v at $\overline{x} = 3/64$ over the $(\overline{y},\overline{z})$ plane for the case of $\hat{u}' \equiv u'/S_L = 1$. Only one scale of spatial variation is apparent when $N = 1$, as expected and illustrated in subplots (a) & (d). However, increasing numbers of disparate spatial scales become apparent with an increase in the number N of fluctuation modes (at constant intensity), as can be seen by comparison of each of the rows of subplots. For example, comparisons of (a) with (b) and (d) with (e) show the effect of an increase from 1 fluctuation mode ($N = 1$) to 2 modes ($N = 2$); while comparisons of (b) with (c) and (e) with (f) show the effect of an increase from 2 fluctuation modes ($N = 2$) to 3 modes ($N = 3$).

SIMULATION PARAMETERS

Selections for the flow strength, number of modes, grid size and rendering method may be made before starting a new simulation run. These parameters are defined as follows.

Strength

Ratio of the intensity of excitation-flow fluctuations to the local, normal surface-propagation speed (e.g., the laminar-flame speed)

Modes

Number of disparate scales of the multiscale excitation flow

Grid Size

Number of nodes in the uniformly spaced 3D grid:

Coarse—32x32x32

Fine—64x64x64

Rendering Method

The method of surface rendering:

MC—Marching Cubes [27]

MC33—Marching Cubes 33 [28]

MC33-C—Marching Cubes 33, Modified [29]

MT—Marching Tetrahedra [30]

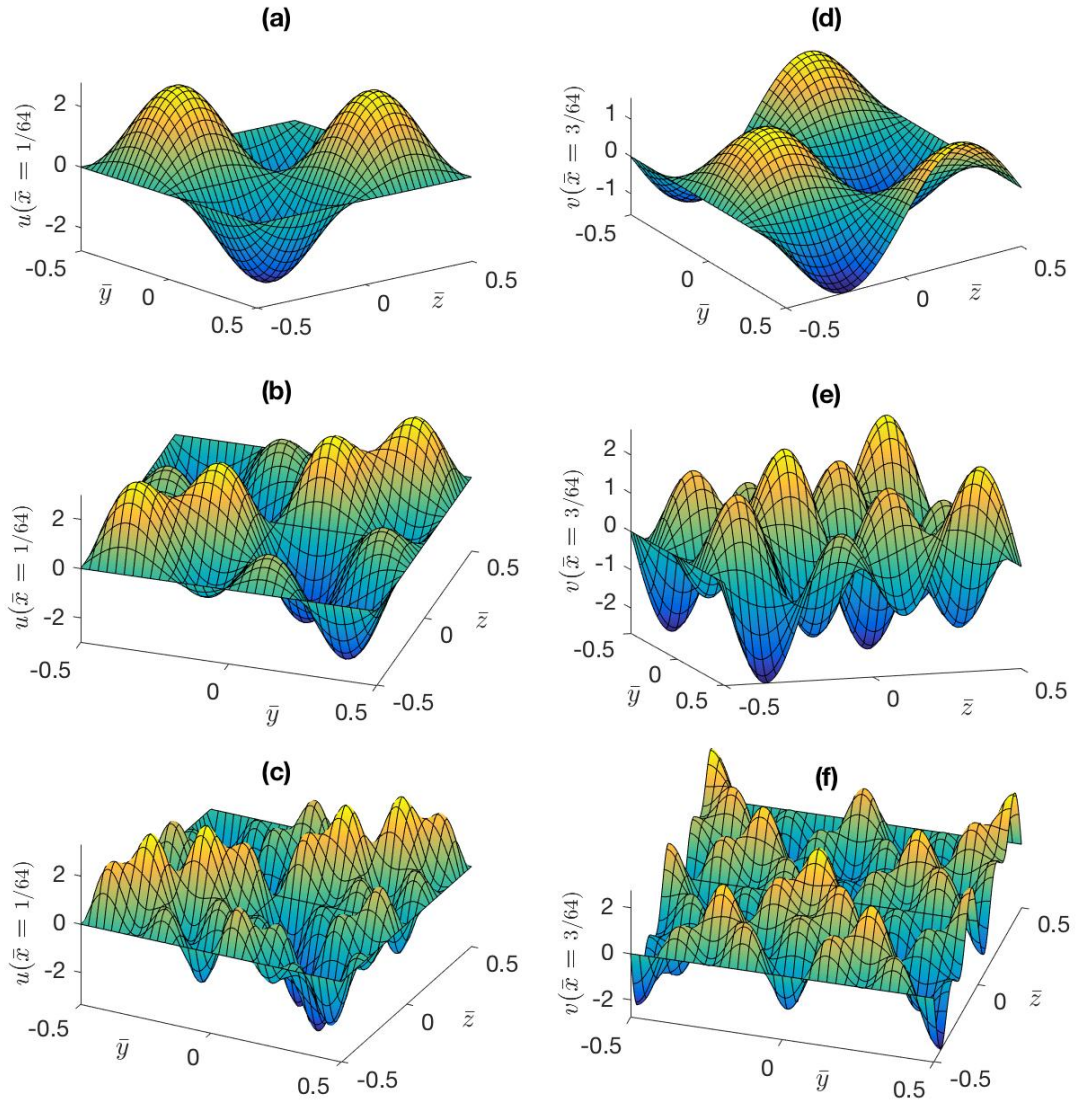

Fig. 1: Excitation-flow distribution with 1 (a & d), 2 (b & e) and 3 (c & f) fluctuation modes

REFERENCES

1. G.H. Markstein and W. Squire, On the Stability of a Plane Flame Front in Oscillating Flow, The Journal of the Acoustical Society of America 27 (1955) 416.
2. V. Bjerknes, J. Bjerknes, H. Solberg and T. Bergeron, Physikalische Hydrodynamik Mit Anwendung Auf Die Dynamische Meterorologie, Verlag von Julius Springer, Berlin, 1933.
3. G.H. Markstein, In: G.H. Markstein (ed), Nonsteady Flame Propagation, The MacMillan Company, New York, 1964.
4. M. Matalon, Intrinsic flame instabilities in premixed and nonpremixed combustion, Annu. Rev. Fluid Mech. 39 (2007) 163-191.
5. F.A. Williams, Combustion Theory, 2nd Ed., Addison-Wesley, Reading, MA, 1985.
6. R.C. Aldredge, The Speed of Isothermal-Front Propagation in Isotropic, Weakly Turbulent Flows, Combustion Science & Technology 178 (2006) 1201-1215.
7. R.C. Aldredge and F.A. Williams, Influence of Wrinkled Premixed-Flame Dynamics on Large-Scale, Low-Intensity Turbulent Flow, Journal of Fluid Mechanics 228 (JUL) (1991) 487-511.

8. A.R. Kerstein, W.T. Ashurst and F.A. Williams, Field equation for interface propagation in an unsteady homogeneous flow field, Physical Review A 37 (7) (1988) 2728.
9. S. Osher and J. Sethian, Fronts propagating with curvature dependent speed: algorithms based on Hamilton-Jacobi formulations, Journal of Computational Physics 79 (1988) 12-49.
10. P. Clavin and F.A. Williams, Effects of molecular diffusion and of thermal expansion on the structure and dynamics of premixed flames in turbulent flows of large scale and low intensity, Journal of Fluid Mechanics 116 (1982) 251-282.
11. G. Joulin and P. Clavin, Linear Stability Analysis of Nonadiabatic Flames: Diffusional-Thermal Model, Combustion and Flame 35 (1979) 139-153.
12. B. Lewis and G. von Elbe, Combustion, Flames and Explosion of Gases, Academic Press, New York, 1961.
13. G.H. Markstein, Proceedings of the Fourth Intl. symp. on Combustion, Williams & Wilkins, Baltimore, 1953, pp. 44-59.
14. P. Clavin and P. Garcia-Ybarra, The influence of the temperature dependence of diffusivities on the dynamics of flame fronts, Journal de Mecanique Appliquee 2 (1983) 245-263.
15. P. Clavin, Dynamic Behavior of Premixed Flame Fronts in Laminar and Turbulent Flows, Progress in energy and combustion science 11 (1985) 1-59.
16. G.I. Sivashinsky, Instabilities, Pattern Formation, and Turbulence in Flames, Annual Review of Fluid Mechanics 15 (1983) 179-199.
17. C.K. Law, Proceedings of the Twenty-Second Symposium (International) on Combustion, The Combustion Institute, Pittsburgh, PA, 1988, pp. 1381-1402.
18. G. Searby and P. Clavin, Weakly turbulent wrinkled flames in premixed gases, Combustion Science and Technology 46 (1986) 167-193.
19. R.C. Aldredge, The Propagation of Wrinkled Premixed Flames in Spatially Periodic Shear Flow, Combustion and Flame 90 (2) (1992) 121-133.
20. S. kwon, L.K. Tseng and G.M. Faeth, Laminar burning velocities and transition to unstable flames in H2/02/N2 and C3H8/02/N2 mixtures, Combustion & Flame 90 (3-4) (1992) 230-246.
21. L.K. Tseng, M.A. Ismail and G.M. Faeth, Laminar Burning Velocities and Markstein Numbers of Hydrocarbon/Air Flames, Combustion & Flame 95 (4) (1993) 410-426.
22. R.C. Aldredge and N.J. Killingsworth, Experimental Evaluation of Markstein-Number influence on Thermoacoustic Instability, Combustion and Flame 137 (2004) 178-197.
23. R.C. Aldredge, Methane-Air Markstein Numbers From Measurements Of Thermoacoustic Instability, Combustion Science & Technology 177 (2005) 1023-1047.
24. M. Matalon, On flame stretch, Combustion Science and Technology 31 (3-4) (1983) 169-181.
25. R.C. Aldredge, Flame-Surface Advection in Transient Periodic Flow, Combustion Science and Technology 187 (1-2) (2015) 148-161.
26. P. Clavin and F.A. Williams, Theory of Premixed-Flame Propagation in Large-Scale Turbulence, Journal of Fluid Mechanics 90 (1979) 589-604.
27. W.E. Lorensen and H.E. Cline, Proceedings of the ACM siggraph computer graphics, ACM, 1987, pp. 163-169.
28. E.V. Chernyaev, Marching cubes 33: Construction of topologically correct isosurfaces, Institute for High Energy Physics, Moscow, Russia, Report CN/95-17 42 (1995)
29. L. Custodio, T. Etiene, S. Pesco and C. Silva, Practical considerations on Marching Cubes 33 topological correctness, Computers & Graphics 37 (7) (2013) 840-850.
30. G.M. Treece, R.W. Prager and A.H. Gee, Regularised marching tetrahedra: improved iso-surface extraction, Computers & Graphics 23 (4) (1999) 583-598.